A MIXTURE FRACTION COMBUSTION MODEL FOR FIRE SIMULATION USING CFD

by

J.E. Floyd, H.R. Baum, and K.B. McGrattan
Building and Fire Research Laboratory
National Institute of Standards and Technology
Gaithersburg, MD 20899, USA

Reprinted from the International Conference on Engineered Fire Protection Design. Proceedings. June 11 – June 15, 2001, San Francisco, CA. Society of Fire Protection Engineers, Bethesda , MD, 279-290 pp, 2001.

National Institute of Standards and Technology
Technology Administration, U.S. Department of Commerce

A MIXTURE FRACTION COMBUSTION MODEL FOR FIRE SIMULATION USING CFD

J.E. Floyd, H.R. Baum, and K.B. McGrattan
Building and Fire Research Laboratory
National Institute of Standards and Technology
100 Bureau Drive Stop 8640
Gaithersburg, MD 20899-8640

INTRODUCTION

The simulation of fires using computational fluid dynamics (CFD) is challenging because it is difficult to couple the combustion chemistry that occurs at very small length scales with the resolvable hydrodynamic field. While it is possible to create a combustion model that tracks the significant species required to calculate the heat release rate, it is too expensive to construct a grid fine enough to resolve individual flame sheets except in cases where the domain is very small. A method, therefore, is needed to model the combustion chemistry in a manner that can be used at the length scales of the resolvable flow field.

One such model, contained in Fire Dynamics Simulator V1.0 (FDS)[1,2], developed at the National Institute of Standards and Technology (NIST), injects Lagrangian "thermal elements" into the flow. These particles, which are convected in the flow field, release energy according to a predefined, time-dependent function. While this method is computationally simple and inexpensive, it lacks the necessary physics to describe underventilated fire scenarios.

The severest restriction of the "thermal element" model is that it requires a user-defined burn-out time, which has been characterized for well-ventilated fires but not for under-ventilated fires. Clearly, a less abstracted method with a better fluid dynamics coupling and a better characterization of oxygen consumption is needed. However, even in the fast chemistry limit, solving equations describing the transport of fuel, oxygen, and the major combustion products would greatly increase the CFD solver's computational requirements. This approach is not necessary, however, as there exists a single quantity that can be used as a surrogate for all of the above. This quantity is the mixture fraction[3], defined as the fraction of the fluid mass that originates as fuel, and from it mass fractions for all other species can be derived based on empirical state relationships.

Typically, a mixture fraction-based combustion model assumes that the reaction is taking place on an infinitely thin flame sheet where both the fuel and oxygen concentrations go to zero. However, since we wish to avoid the expense of resolving the flow field at length scales fine enough to capture the actual flame sheet location, the traditional mixture fraction-based model is modified to allow for a reaction zone of finite thickness. These modifications preserve the original chemical equation for the combustion process as well as provide a framework for the inclusion of minor combustion species.

A mixture fraction-based combustion model has been incorporated into FDS. Comparisons between the new combustion model for FDS, the old combustion model, and a variety of test cases demonstrate the value of the new model. These test cases include a simple fire plume and a small compartment.

MIXTURE FRACTION MODEL

FDS solves the "low Mach number" form of the Navier-Stokes equations[4] for a multiple species fluid. These equations are obtained by filtering out pressure waves from the Navier-Stokes equations, resulting in a set of conservation equations valid for low-speed, buoyancy driven flow. These equations allow for large variations in density but not pressure. These equations are discretized in space using second order central differences and in time using an explicit, second order, predictor-corrector scheme.

For very small scale fires, such as a small Bunsen burner, it is feasible to create a simulation capable of being run on a modestly powered computing platform that is detailed enough in both length scales and time scales to directly capture the combustion processes. However for the large scale problems of interest to the fire safety community this is not feasible. A typical compartment fire involves length scales of meters and time scales of minutes. To create a simulation of a typical compartment fire at the resolution of a Bunsen burner could be done with an extremely powerful supercomputer; however, this would be of little practical use. Instead we must approximate the combustion process in both space and time.

One simple method of coupling the combustion process with the flow field is to track three species: fuel, oxygen, and nitrogen. Since the time scales of the convective processes are much longer than the time scales of the combustion processes, infinite reaction rate chemistry can be assumed. Note, however, that this method requires solving for three species and that more species would be required to handle combustion products.

The observation can be made, however, that to track both fuel and oxygen when assuming an infinite reaction rate is redundant if the local temperature is not considered. Since neither fuel nor oxygen can coexist under those assumptions, if fuel is present there can be no oxygen and vice-versa. Thus, the above method could be simplified further by replacing all the species with a single species that represents the amount of fuel or oxygen present in any given location.

One scalar parameter that can be used to represent the local concentration of fuel or oxygen is the mixture fraction. If F is defined as fuel, O is defined as oxygen, Y is defined as a mass fraction, Y_O^∞ as the ambient oxygen mass fraction, and Y_F^I as the fuel mass fraction in the fuel stream, the mixture fraction, Z, is defined as[5]:

$$Z = \frac{sY_F - \left(Y_O - Y_O^\infty\right)}{sY_F^I + Y_O^\infty}; \quad s = \frac{\upsilon_O w_O}{\upsilon_F w_F} \tag{1}$$

In its traditional implementation, mixture fraction chemistry assumes that fuel and oxygen cannot co-exist. That is, it uses an infinite reaction rate and assumes that fuel and oxygen will react at

any temperature. Thus the mixture fraction at all points in the computational domain, in essence represents a 'post-combustion' value, i.e. only products are present at any location in the computational domain. This is more easily seen in the following. Assume that a generic hydrocarbon fuel is being burned. The complete stoichiometric reaction for this is:

$$C_xH_y + \left(x + \tfrac{y}{4}\right)(O_2 + 3.76N_2) \rightarrow xCO_2 + \tfrac{y}{2}H_2O + \left(x + \tfrac{y}{4}\right)3.76N_2 \tag{2}$$

If we allow for conditions where the available oxygen is non-stoichiometric, that is the available oxygen is some fraction, ξ where ξ varies from 0 to ∞, of the required amount and assume ideal combustion, then Equation 2 becomes:

$$\begin{aligned} C_xH_y + \xi\left(x + \tfrac{y}{4}\right)(O_2 + 3.76N_2) \rightarrow \mathrm{Max}[0, 1-\xi]C_xH_y + \mathrm{Min}[1, \xi]xCO_2 \\ +\mathrm{Min}[1, \xi]\tfrac{y}{2}H_2O + \mathrm{Max}[0, (\xi - 1)]O_2 + \xi\left(x + \tfrac{y}{4}\right)3.76N_2 \end{aligned} \tag{3}$$

Using Equation 1, the mass fractions of the products in Equation 3 can be plotted as a function of Z. As ξ varies from ∞ to 0, Z will vary from 0 to 1, and a series of state relationships for the species can be expressed in terms of the mixture fraction. In this manner the mixture fraction, as one species, can be used to represent many species in the simulation. For example, if the fuel is assumed to be methane, the state relationships shown in Figure 1 are obtained.

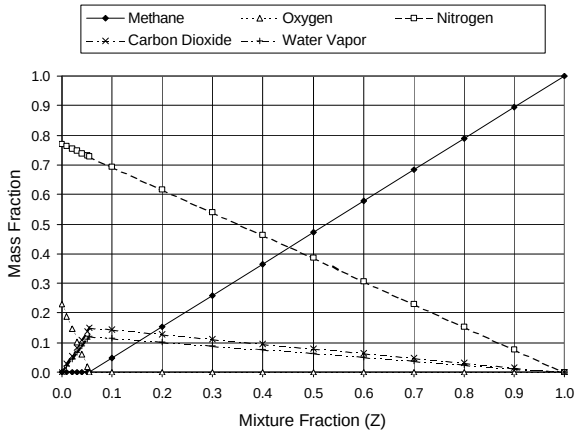

Figure 1: Methane State Relations

With this representation the flame sheet is defined to exist at the point where both fuel and oxygen disappear as products. The mixture fraction corresponding to this point is designated Z_F and this point is equivalent to the reaction shown in Equation 2. This region is a two dimensional surface, and for larger scale simulations is difficult to resolve. To implement the mixture fraction an expression for the local heat release rate as a function of the mixture fraction must be developed.

This is done rather simply. Combustion of fuel consumes oxygen. Since the mixture fraction yields information about the local oxygen concentration, we need only determine an expression for the oxygen consumption rate based on the mixture fraction. Then using the heat of combustion yields the local heat release rate. Consider the transport equations for the conserved scalar Z and for oxygen where D is the turbulent diffusion coefficient, ρ is the density, and $\dot{m}_O$ is the mass rate of change of oxygen at a location, e.g. oxygen consumption during combustion.

$$\rho\frac{DZ}{Dt} = \nabla \cdot \rho D \nabla Z \tag{4}$$

$$\rho\frac{DY_O}{Dt} = \nabla \cdot \rho D_O \nabla Y_O + \dot{m}_O \tag{5}$$

The derivatives for oxygen in Equation 5 are expressed in terms of mixture fraction using the chain rule, diffusion is assumed constant with respect to species, and Equation 4 is multiplied by $\frac{dY_O}{dZ}$.

$$\rho \frac{dY_O}{dZ} \frac{DZ}{Dt} = \frac{dY_O}{dZ} \nabla \cdot \rho D \nabla Z \tag{6}$$

$$\rho \frac{dY_O}{dZ} \frac{DZ}{Dt} = \nabla \cdot \rho D \frac{dY_O}{dZ} \nabla Z + \dot{m}_O \tag{7}$$

Equation 6 is subtracted from Equation 7.

$$-\dot{m}_O = \nabla \cdot \rho D \frac{dY_O}{dZ} \nabla Z - \frac{dY_O}{dZ} \nabla \cdot \rho D \nabla Z \tag{8}$$

With Equation 8 one can now determine the local mass loss rate of oxygen as a function of the mixture fraction. By making use of vector differentiation identities, Equation 8 can be simplified into the following form which shows that oxygen is only consumed and not produced.

$$-\dot{m}_O = \rho D \frac{d^2 Y_O}{dZ^2} (\nabla Z)^2 \tag{9}$$

At first glance, Equation 8 appears to be rather complex. However, its meaning can be understood simply. It can be seen in Figure 1 that $\frac{dY_O}{dZ}$ at any point in the computational domain is either zero or a constant depending on which side of Z_F one is located. If the computational domain is divided into the two regions of $Z \leq Z_F$ and $Z > Z_F$, then Equation 8 can be integrated over these two regions while applying the divergence theorem. Since the $\frac{dY_O}{dZ}$ term will be zero in the region $Z > Z_F$, this region can be ignored. The end result is the mass loss rate of oxygen as a function of the mixture fraction diffusion across the flame surface as shown below:

$$\int \dot{m}_O \, \partial V = -\frac{dY_O}{dZ} \int_{Z=Z_F} \rho D \nabla Z \cdot \vec{n} \, \partial S \tag{10}$$

Since oxygen is a function of only the mixture fraction, this is equivalent to saying that the global heat release rate is a function of the oxygen gradient across the flame sheet. In fact due to the diffusion constant in the expression and the assumption of infinite reaction rates, Equation 10 states that the heat release rate is due solely to the diffusion of oxygen across the flame, which is given by the hydrodynamic solver. Since we do not know a priori the location of the flame sheet, and since the $\frac{d^2 Y_O}{dZ^2}$ term in Equation 9 is a δ-function, only Equation 8 is useful for a numerical scheme.

ADDITIONAL CODE MODIFICATIONS

FDS v1.0 computes radiative fluxes with a Monte-Carlo style ray-tracing from the burning particles to the walls. The model neglects gas to gas and wall to wall interaction, and thus, does not fare well with compartment scenarios with very hot gas layers or surfaces. The original Monte-Carlo style radiation model was changed to a Finite Volume Method[6]. This method is derived from the radiative transport equation for a non-scattering gray gas.

$$\hat{s} \cdot \nabla I(x, \hat{s}) = \kappa(x)[I_b(x) - I(x, \hat{s})] \tag{12}$$

$I(x,\hat{s})$ is the radiation intensity, $I_b(x)$ is the blackbody radiation intensity, $\kappa(x)$ is the absorption coefficient, and $\hat{s}$ is the unit normal direction vector. Implementing this equation in a large eddy simulation requires determining how to specify the absorption coefficient, κ, and how to create the source term $I_b(x)$. Currently a number of methods for both are being examined. For the purpose of these simulations $\kappa(x)$ is given by a mass fraction weighted, linear combination of the optically thin mass extinction coefficients, σ, for soot[7], fuel, CO_2, and water vapor[8] as shown below:

$$\kappa = (Y_{soot}\sigma_{soot} + Y_{Fuel}\sigma_{Fuel} + Y_{CO_2}\sigma_{CO_2} + Y_{H_2O}\sigma_{H_2O})\rho \tag{13}$$

This means that $\kappa(x)$ is a function of the mixture fraction. Soot, due to its large absorption coefficient, quickly becomes a dominating component in $\kappa(x)$. Determining a manner in which to ensure a correct source term regardless of grid size is an issue yet to be solved. This difficulty arises since in a typical calculation grid cells with combustion are not at the flame temperature since the flame only makes up a small fraction of the cell volume.

COMPARISONS OF OLD VS NEW COMBUSTION ROUTINE

The new combustion routine has been tested with a variety of fire scenarios. A few are shown here and compared with the old combustion routine, referred to as the “thermal element method”.

Pool Fire

Simulations of an 0.2 m diameter pool fire was performed for three different fire sizes: 14 kW, 24 kW, and 62 kW. With a grid size over the burner of 0.027 cm. This grid size was chosen to meet the requirements of the flow solver [9]. Once a steady-state was reached, time averages were taken of the centerline temperatures and vertical velocities. These were compared with temperatures and velocities calculated using McCaffrey’s correlation[10].

Figures 2 and 3 shown below illustrate some of the major improvements that arise from the use of the mixture fraction. Since the “thermal elements” are transported solely by the velocity field and since the normal velocity at a surface is essentially zero it takes the particles time to move away from the burner. As a result a large fraction of the particle’s heat is emitted incorrectly near

the burner surface. Since, the mixture fraction is transported by both advection and diffusion, the heat release occurs above the burner surface as expected with this new method. Furthermore, the requirement that combustion occurs on the Z_F surface results in the heat being released towards the edge of the plume where the oxygen is located. In contrast the thermal particles which move towards the center of the plume due to the radial entrainment velocity, release their heat towards the plume center.

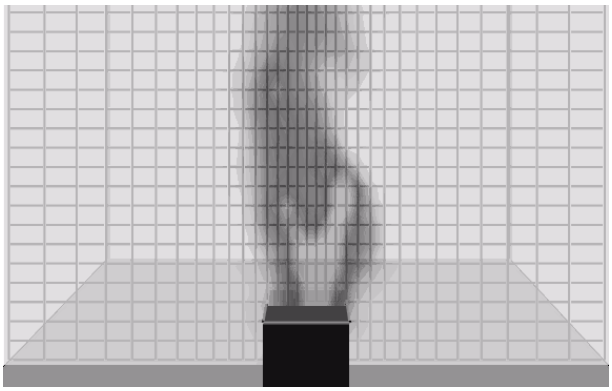

Figure 2: 62 kW FDS 1.0 Temperature

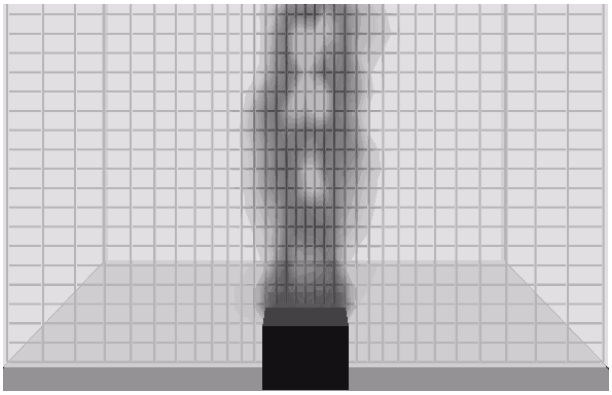

Figure 3: 62 kW FDS New Temperature

Figures 4 through 9 display the results of these simulations vs. McCaffrey's Correlation.

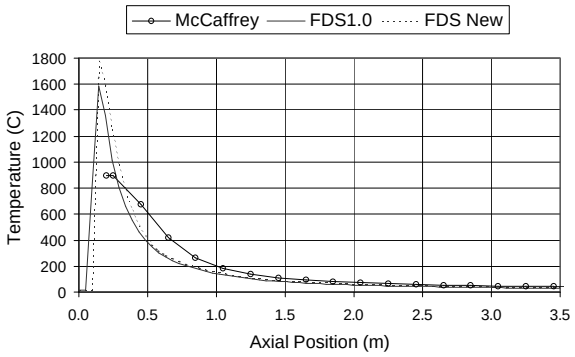

Figure 4: 14 kW Axial Temperature Profile

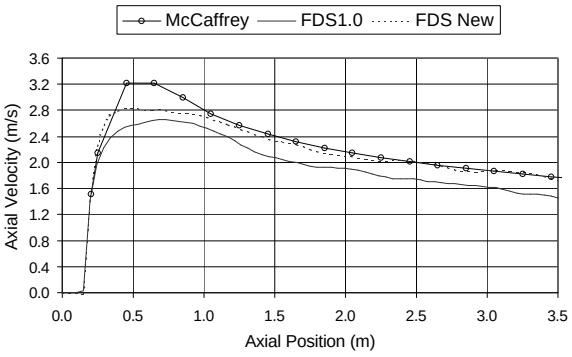

Figure 5: 14 kW Axial Velocity Profile

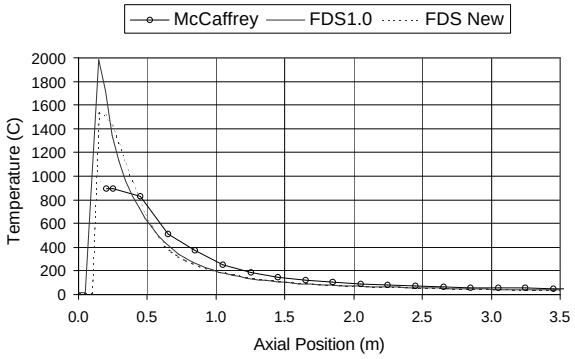

Figure 6: 24 kW Axial Temperature Profile

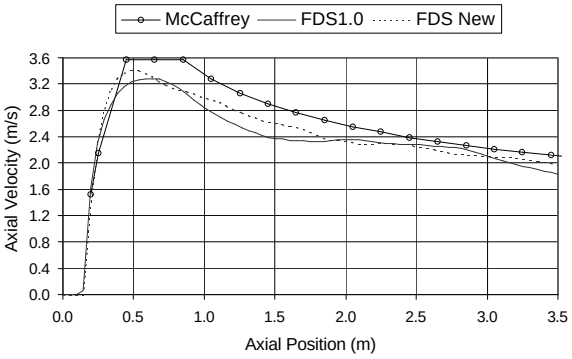

Figure 7: 24 kW Axial Velocity Profile

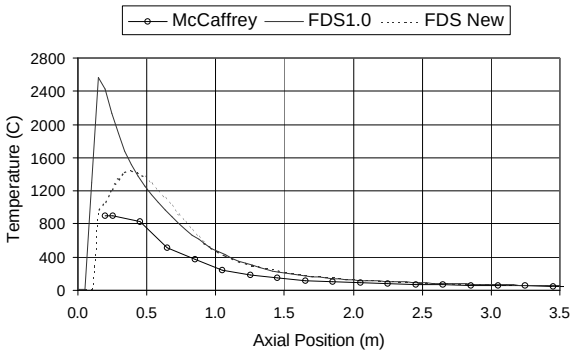

Figure 8: 62 kW Axial Temperature Profile

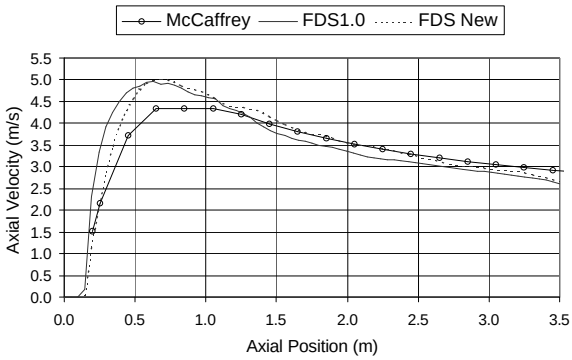

Figure 9: 62 kW Axial Velocity Profile

The following observations are made:

1. Far-field temperature predictions for both methods are the same and agree with McCaffrey's correlation. This is to be expected since the far-field calculation is driven by buoyancy forces which depend upon the total heat release rate rather than its spatial distribution.
2. As the fire power increases, the near-field temperatures for the mixture fraction improves. This results from a better resolution of the mixture fraction gradient and a more accurate prediction of the spatial heat release as the surface Z_F moves out of the first grid cell. At low heat release rates on the other hand the mixture fraction model results in combustion only in the first grid cell above the burner for the coarse grid used in the computation. This shortcomming should not be taken as an indictment of the mixture fraction method. With a more resolved grid, this would not be the case. For example increasing the number of grid cells by 40% results in a 12% drop in the maximum centerline temperature.
3. Velocity predictions show an improvement relative to McCaffrey's correlation for the mixture fraction model for all fire sizes.

NIST-BFRL 40% Reduced Scale Enclosure

A recent investigation at NIST attempted to determine the measurement uncertainties in the use of bare-bead and aspirated thermocouples for compartment fires[11]. As part of this investigation, natural gas and hexane fires were set inside of a 40% scale compartment based on a proposed ISO standard (ISO-9705). A 100 kW natural gas fire was selected from this investigation for simulation with FDS. This test was selected to avoid adding further predictive uncertainties that would result from choosing an underventilated test as it is already known that FDS v1.0 is less accurate in underventilated scenarios and this would make comparison of the two combustion models difficult. The compartment and the measurement locations chosen for simulation are shown in Figure 10. The gas burner was located in the center of the compartment with its top 0.15 m above the floor. For the simulations the grid size was 0.04 m and the computational domain was extended beyond the doorway by one third of the compartment's length. The simulation results are compared with data collected during the 100 kW test.

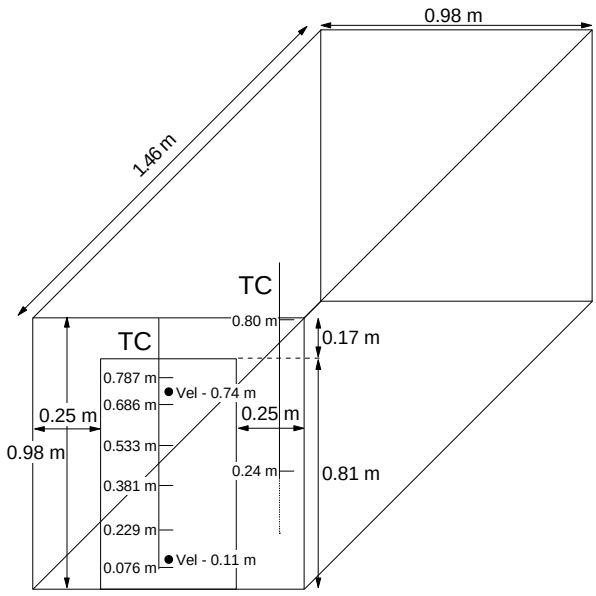

Figure 10: 40% Reduced Scale Enclosure

Figures 11 and 12, below, show predicted vs. measured temperatures for the two aspirated thermocouples (TC) located at 0.24 m and 0.80 m inside the front of the compartment. A few observations are made from these figures:

1. At the start of the fire both models show much faster temperature increases than measured during the test. This is probably due in part to numerical diffusion of heat since coarse grid was used.
2. For the upper TC, FDS v1.0 overpredicts the temperature increase by 14% at this location whereas the new model underpredicts the increase by 25%. The overprediction by FDS v1.0 is primarily a result of the radiation model which does not calculate radiative transfer from the ceiling layer to the floor. The underprediction of the new model has two possible contributions. One, the heat release distribution with respect to the flow field may result in less of the fire plume impinging on the thermocouple. Two, the new models may be overpredicting the wall and radiative losses from the hot gas.
3. For the lower TC, after 40 s FDS v1.0's predictions lie below the measured data. The predictions of the new model agree well with the measurements over this time period. These results are primarily due to the different radiation models.

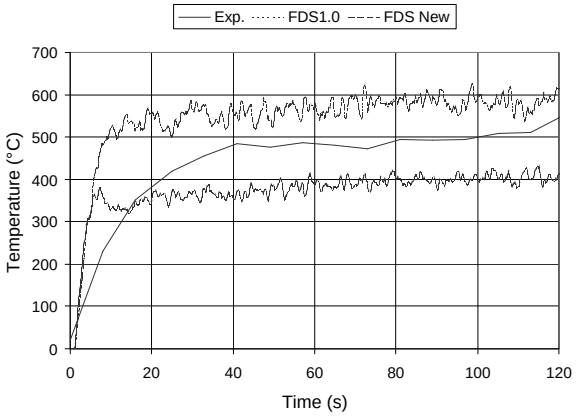

Figure 11: 0.80 m Compartment TC

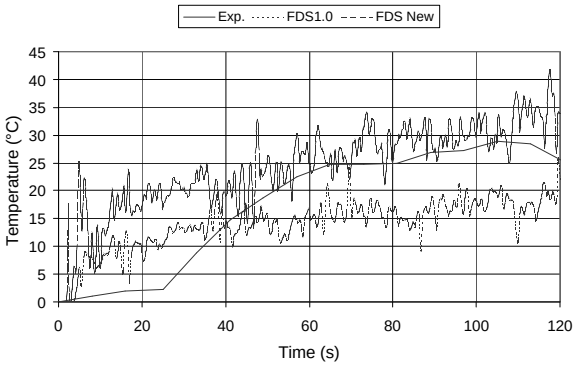

Figure 12: 0.24 m Compartment TC

Figures 13 and 14, shown below, plot the predicted and measured velocities in the doorway. The measurements were made by bi-directional probes. At both locations, the velocity predictions differ from one another by approximately 10% and the difference is in the direction of the temperature difference. At the lower probe the predictions lie between the measured data and at the upper probe the predictions lie about 20% below the measured data. Again it is observed that both versions of FDS show a faster initial transient.

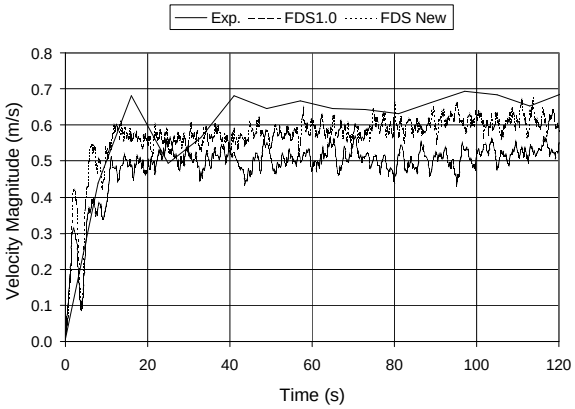

Figure 13: 0.11 m Doorway Velocity

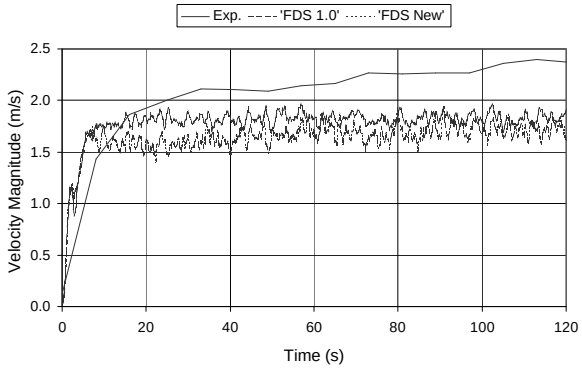

Figure 14 0.74 m Doorway Velocity

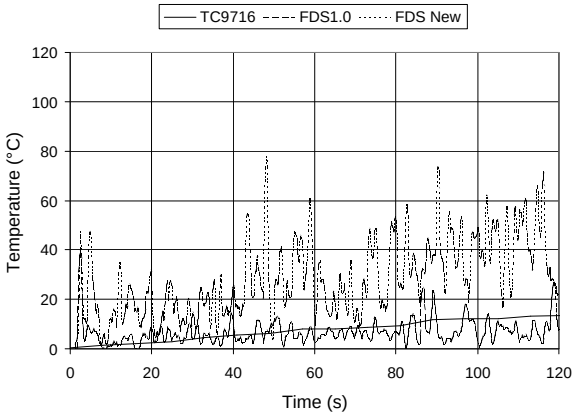

Figure 15: 0.381 m Doorway TC

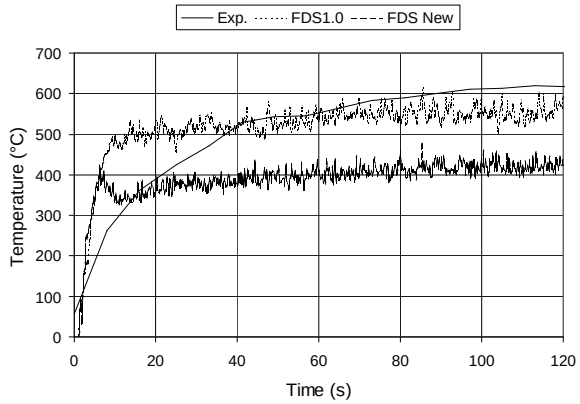

Figure 16: 0.787 m Doorway TC

The final three comparisons for this scenario are shown in Figures 15 through 17. These figures are for two TC's in the doorway, near the middle at 0.381 m and near the top at 0.787 m, and for the doorway temperature profile at 120 s.

From these figures it is clear that neither version of FDS appears to be correctly predicting the temperatures at the lowest elevations. However, the newer model does result in an improved prediction. At the highest elevations both models underpredict the measured data, with the new model underpredicting by 30%. The doorway temperature profile indicates that the old model predicts a similar shape to the profile with the layer height lying below the measured layer height. The new model shows a broader, but flatter temperature profile in the doorway indicating that the new model is resulting in additional mixing between the layers causing the upper layer to grow downward and decrease in temperature.

Virginia Tech 50% Reduced Scale Enclosure

The Virginia Tech Fire Research Lab is currently investigating the formation and transport mechanisms for CO using a 50% scale version of the ISO-9705 compartment[12], a slightly larger version of the NIST compartment from the previous section. Figure 18 shows the overall

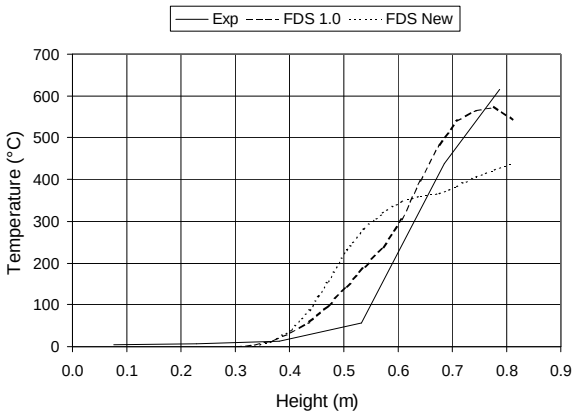

Figure 17: Doorway Temperature Profile

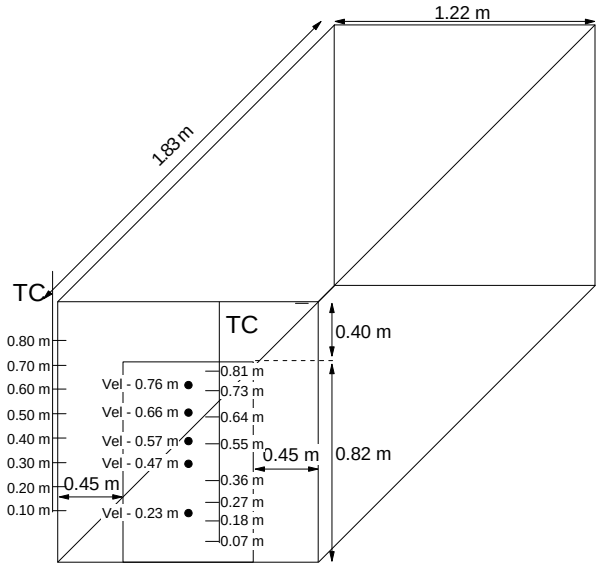

Figure 18: 50% Reduced Scale Enclosure

compartment geometry and sensor locations for the Virginia Tech (VT) enclosure. Fires in this compartment are from a 30 cm diameter propane burner located in the center of the compartment. Temperature measurements are from aspirated thermocouples and velocity measurements are from bi-directional probes. As with the NIST compartment a small fire, 126 kW, was selected for simulation using a grid size of 0.04 m with the domain extended beyond the doorway by one third of the compartment's length.

Table 1 shows a side-by-side comparison of the experimental results and the two FDS simulations. The results are shown three minutes after ignition of the burner. Results are shown for the 8 TC's inside the front corner of the fire room, the 8 TC's on the right side of the doorway, and the 5 velocity probes located along the center line of the doorway**.**

The two versions of FDS show similar predictive outcomes for the VT enclosure as for the NIST enclosure with both version showing similar temperatures near the floor and both versions underpredicting the upper temperatures. However, for the VT enclosure the predicted upper layer temperatures are closer to each other than for the NIST enclosure. It is also observed that both versions predict a lower layer interface height than observed experimentally. Temperature predictions in the doorway show similar trends; however, the new FDS predictions are closer to the measured data than for the NIST enclosure. In the doorway, velocity predictions are nearly identical for both versions of FDS and correlate well with the lower doorway data. In the upper doorway the velocities are not as well predicted with both versions being about 50% low in their predictions.

CONCLUSIONS

A new combustion model has been added to FDS v1.0 to test the mixture fraction approach to simulate combustion. This new model was tested against three different scenarios and the results compared to both the old "thermal element" model as well as available experimental data.

Table 1: Results of Simulating a 126 kW Propane Fire in the Virginia Tech 50% RSE

Parameter	Units	Experiment	FDS 1.0	New Model
Fire Room TC 10 cm	$T-T_0$ °C	150	35	44
Fire Room TC 20 cm	$T-T_0$ °C	154	71	77
Fire Room TC 30 cm	$T-T_0$ °C	312	121	171
Fire Room TC 40 cm	$T-T_0$ °C	471	206	368
Fire Room TC 50 cm	$T-T_0$ °C	565	372	464
Fire Room TC 60 cm	$T-T_0$ °C	585	471	494
Fire Room TC 70 cm	$T-T_0$ °C	605	512	513
Fire Room TC 80 cm	$T-T_0$ °C	612	542	531
Doorway TC 7 cm	$T-T_0$ °C	12	0	0
Doorway TC 18 cm	$T-T_0$ °C	16	0	0
Doorway TC 27 cm	$T-T_0$ °C	20	21.2	20.8
Doorway TC 36 cm	$T-T_0$ °C	54.9	145	112
Doorway TC 55 cm	$T-T_0$ °C	468	363	445
Doorway TC 64 cm	$T-T_0$ °C	539	418	503
Doorway TC 73 cm	$T-T_0$ °C	524	464	516
Doorway TC 81 cm	$T-T_0$ °C	410	454	528
Doorway Vel 23 cm	m/s	-0.58	-0.59	-0.58
Doorway Vel 47 cm	m/s	1.09	0.72	1.01
Doorway Vel 57 cm	m/s	2.58	1.25	1.62
Doorway Vel 66 cm	m/s	3.88	1.92	2.03
Doorway Vel 76 cm	m/s	5.22	2.86	2.96

The first scenario was a pool fire in the open. Slight improvements were seen in velocity and temperature predictions in the far-field with the new model. In the near-field, the new model was an improvement for larger pool fires. For the small pool fire, the mixture fraction method, which relies on a concentration gradient to determine heat release, predicted too small of a combustion zone which resulted in a perturbed near-field temperature distribution.

The second scenario was a 100 kW methane fire in the NIST 40% reduced scale enclosure. Results for this case were mixed with the mixture fraction model yielding better results in the lower layer, but poorer results in the upper layer. It is quite likely that further development to radiation heat transfer may result in an improved upper layer prediction. This work is needed to determine the appropriate absorption coefficients to use for the calculations as well as how to define the source term on coarse grids where flame temperatures are not reached.

The third scenario was a 126 kW test in the VT 50% reduced scale enclosure. For this scenario the mixture fraction model was overall a slight improvement over the old “thermal element” model. As with the NIST enclosure, it is possible that improvements to the radiation model may result in better upper layer predictions by the mixture fraction model.

The mixture fraction combustion model was successfully implemented in FDS. This new model yields slight improvements in the predictive capabilities of the code for the cases tested. However, this is not its only benefit. The “thermal elements” were in essence an over simplified method of tracking fuel. Replacing the “thermal elements” with the mixture fraction adds more

information on chemistry and some additional information on fuel transport. Since the mixture fraction solves the species conservation equation and the "thermal elements" do not. Also, the mixture fraction, as a single species, through its state relationships, see Figure 1, contains information about combustion products. Thus, with the mixture fraction, FDS can now track multiple species for the same cost as the "thermal element" model when used with oxygen depletion. Lastly, the "thermal element" model has only a rudimentary capability to handle underventilated combustion. The mixture fraction model is only limited by one's ability to define a state relationship for the combustion products. It is hoped that the current idealized combustion can be expanded to include minor species such as soot and CO. Therefore, with the mixture fraction approach, FDS has the potential to better account for unburned fuel and oxygen without the addition of a great deal of complexity and computational time. It appears, however, that this does come at the price of requiring denser grids for very small fires. Further work is still needed to resolve grid dependent issues in the radiation solver and to determine the local rate of combustion.

REFERENCES

1. McGrattan, K., et al., "Fire Dynamics Simulator - Technical Reference Guide", National Institute of Standards and Technology, NISTIR 6467, 2000.
2. McGrattan, K. And Forney, G., "Fire Dynamics Simulator - User's Manual", National Institute of Standards and Technology, NISTIR 6469, 2000.
3. Mell, W., McGrattan, K., and Baum, H., "Numerical Simulation of Combustion in Fire Plumes", Proceedings of the 26th International Symposium on Combustion, Combustion Institute, 1996, pp. 1523-1530.
4. Rehm, R. And Baum, H., "The Equations of Motion for Thermally Driven, Buoyant Flows" Journal of Research of the NBS, Vol. 83, 1978, pp. 297-308.
5. Mahalingam, S., et al., "Analysis and Numerical Simulation of a Nonpremixed Flame in a Corner", Combustion and Flame, Vol. 118, 1999, pp. 221-232.
6. Raithby, G. and Chui, E. "A Finite-Volume Method for Predicting Radiant Heat Transfer in Enclosures with Participating Media", Journal of Heat Transfer, Vol. 112, 1990, pp. 415-423.
7. Mulholland, G. And Choi, M., "Measurement of the Mass Specific Extinction Coefficient for Acetylene and Ethene Smoke Using the Large Agglomerate Optics Facility", The Combustion Institute, 27th Symposium on Combustion, 1998, pp. 1515-1522.
8. Grosshandler, W., "RADCAL: A Narrow-Band Model for Radiation Calculations in a Combustion Environment," National Institute of Standards and Technology, NIST Technical Note 1402, 1993.
9. Baum, H., et al., "Three Dimensional Simulations of Fire Plume Dynamics", Proceedings of the 5th International IAFSS Symposium, Fire Safety Science, 1997, pp. 511-522.
10. Karlsson, B. And Quintiere, J., "Enclosure Fire Dynamics", CRC Press, 2000.
11. Pitts, W., et al., "Temperature Uncertainties for Bare-Bead and Aspirated Thermocouple Measurements in Fire Environments", Proceedings of the 14th Meeting of the UJNR Panel on Fire Research, 1998.
12. Wieczorek, C., et al., "Species Formation Using n-Hexane Fires in a Scaled ISO Compartment", NIST Annual Conference on Fire Research, 1998, pp. 103-104.